

# Cyanide — a Strong Field Ligand for Ferrohemes and Hemoproteins? \*\*

## Supporting Information

Jianfeng Li, Richard L. Lord, Bruce C. Noll, Mu-Hyun Baik, Charles E. Schulz, and W. Robert Scheidt\*

August 20, 2008

[★] Dr. Jianfeng Li, Dr. Bruce C. Noll, Prof. W. Robert Scheidt

Department of Chemistry and Biochemistry  
University of Notre Dame, Notre Dame, Indiana 46556 (USA)  
Fax (574) 631-6652  
E-mail: Scheidt.1@nd.edu

Prof. Charles E. Schulz  
Department of Physics, Knox College  
Galesburg, Illinois 61401 (USA)

Richard L. Lord, Prof. Mu-Hyun Baik  
Department of Chemistry  
Indiana University, Bloomington, Indiana 47405 (USA)

[★★] We thank the National Institutes of Health for support  
of this research under Grant GM-38401 to WRS and  
the NSF for X-ray instrumentation (Grant CHE-0443233)

Supporting information for this article is available on the WWW  
under <http://www.angewandte.org> or from the author.

## Experimental Section

**General Information.** All reactions and manipulations were carried out under argon using a double-manifold vacuum line, Schlenkware and cannula techniques. Benzene, THF and hexanes were distilled over sodium/benzophenone and dichloromethane over CaH<sub>2</sub>. Chlorobenzene was washed with concentrated sulfuric acid, then with water until the aqueous layer was neutral, dried with MgSO<sub>4</sub>, and distilled twice over P<sub>2</sub>O<sub>5</sub> under argon. KCN was recrystallized and purified by a literature procedure.<sup>1</sup> Ethanethiol and Kryptofix 222 (Aldrich) were used as received. The free-base porphyrin ligand *meso*-tetraphenylporphyrin (H<sub>2</sub>TPP) were prepared according to Adler et al.<sup>2</sup> [Fe(TPP)]<sub>2</sub>O was prepared according to a modified Fleischer preparation.<sup>3</sup> IR spectra were recorded on a Nicolet Nexus 670 FT-IR spectrometer as KBr pellets. Mössbauer measurements were performed on a constant acceleration spectrometer from 25 K to 300 K with optional small field (Knox College). Samples for Mössbauer spectroscopy were prepared by immobilization of the crystalline material in Apiezon M grease.

**Synthesis of [K(222)][Fe(TPP)(CN)].** [Fe(II)(TPP)] was prepared by reduction of [Fe(TPP)]<sub>2</sub>O (27.1 mg, 0.02 mmol) with ethanethiol (0.5 mL) in benzene (8 mL) for 24 hours. Vacuum evaporation of the solvent yielded a dark purple solid to which KCN (2.9 mg, 0.044 mmol) and Kryptofix 222 (16.6 mg, 0.044 mmol) in THF or PhCl was added by cannula and the mixture was stirred overnight. X-ray quality crystals were finally obtained in 8 mm × 250 mm sealed glass tubes by liquid diffusion using hexanes as non-solvent. Very strong C≡N stretches were found for iron(II) cyanide porphyrinates compared to the iron(III) analogues which are much weak.<sup>4</sup> IR  $\nu_{C\equiv N}$ : 2070, 2105 cm<sup>-1</sup>.

**X-ray Structure Determinations.** Single crystal experiments were carried out on a Bruker Apex system with graphite monochromated Mo K $\alpha$  radiation ( $\lambda = 0.71073 \text{ \AA}$ ). The crystalline samples were operated by certain method described below. The structures were solved by direct methods using SHELXS-97<sup>5</sup> and refined against  $F^2$  using SHELXL-97;<sup>6, 7</sup> subsequent difference Fourier syntheses led to the location of most of the remaining non-hydrogen atoms. For the structure refinement all data were used including negative intensities. All nonhydrogen atoms were refined anisotropically if not remarked otherwise below. Hydrogen atoms were idealized with the standard SHELXL-97 idealization methods. The program SADABS<sup>8</sup> was used to apply an absorption correction. Complete crystallographic details,

atomic coordinates, anisotropic thermal parameters, and fixed hydrogen atom coordinates are given in the Supporting Information for the two structures.

**[K(222)][Fe(TPP)(CN)] (100, 296, 325, 400K).** A dark purple crystal with the dimensions  $0.55 \times 0.35 \times 0.35$  mm<sup>3</sup> was used for the temperature-dependent structure determination. The crystal was mounted in a sealed capillary. Measurement temperature is 100, 296, 325 and 400 K respectively. The asymmetric unit contains one porphyrin complex and one potassium cation coordinated with Kryptofix 222. All the atoms are ordered and no solvent molecule was found.

**Magnetic Measurements.** Magnetic susceptibility measurements were obtained on ground samples in the solid state over the temperature range 2-400 K on a Quantum Design MPMS SQUID susceptometer. The samples were loaded in an inert atmosphere glovebox in a sealed holder. Measurements at two fields (2000 and 20000 Gauss) showed that no ferromagnetic impurities were present; duplicate measurements ensured reproducibility among different sample preparations.  $\chi_M$  was corrected for the porphyrin ligand diamagnetism according to previous experimentally observed values;<sup>9</sup> all remaining diamagnetic contributions were calculated using Pascal's constants;<sup>10</sup> A value of  $-7.654 \times 10^{-4}$  cm<sup>3</sup>/mol was used for [K(222)][Fe(TPP)(CN)]. All measurements included a correction for the diamagnetic sample holder. All magnetic data were also corrected for temperature-independent paramagnetism (TIP) value of  $1.3 \times 10^{-3}$  cm<sup>3</sup>/mol.

**Computational Details.** All calculations were carried out using Density Functional Theory as implemented in the Jaguar 7.0 suite of quantum chemistry programs.<sup>11</sup> Geometry optimizations were performed at the B3LYP/6-31G\*\* level of theory,<sup>12</sup> with Fe represented using the Los Alamos LACVP basis which includes effective core potentials.<sup>13</sup> Independent studies demonstrated that B3LYP over-stabilizes high spin electron configurations,<sup>14</sup> thus, the energies were reevaluated using Dunning's correlation-consistent triple- $\zeta$  basis set cc-pVTZ(-f)<sup>15</sup> at the optimized geometry with the B3LYP\* functional<sup>6b</sup> prescribed by Reiher and co-workers. For Fe, we use a modified version of LACVP, designated as LACV3P, where the exponents were decontracted to match the effective core potential with a triple- $\zeta$  quality basis. All stationary points were confirmed to be minima by checking the harmonic frequencies. Thermodynamic properties were calculated as summarized below, where we assume standard

approximations for deriving the entropy corrections in gas phase.

$$\Delta H(\text{gas}) = \Delta E(\text{SCF}) + \Delta ZPE \quad (1)$$

$$\Delta G(\text{gas}) = \Delta H(\text{gas}) - T\Delta S(\text{gas}) \quad (2)$$

$\Delta H(\text{gas})$  = gas phase enthalpy;  $\Delta E(\text{SCF})$  = electronic energy computed in the self-consistent-field calculation;  $\Delta ZPE$  = zero-point energy correction (using unscaled frequencies);  $\Delta G(\text{gas})$  = gas phase Gibbs free energy;  $\Delta S(\text{gas})$  = gas phase entropy (using unscaled frequencies);  $\Delta G(\text{sol})$  = solution phase free energy;  $\Delta G_{\text{sol}}$  = free energy of solvation.

## References and Notes

- (1) Armarego, W. L. F.; Perrin, D. D. *Purification of Laboratory Chemicals* **1997**, Fourth Edition, 413.
- (2) Adler, A. D.; Longo, F. R.; Finarelli, J. D.; Goldmacher, J.; Assour, J.; Korsakoff, L. *J. Org. Chem.* **1967**, 32, 476.
- (3) (a) Fleischer, E. B.; Srivastava, T. S. *J. Am. Chem. Soc.* **1969**, 91, 2403. (b) Hoffman, A. B.; Collins, D. M.; Day, V. W.; Fleischer, E. B.; Srivastava, T. S.; Hoard, J. L.; *J. Am. Chem. Soc.* **1972**, 94, 3620.
- (4) Li, J.; Noll, B. C.; Schulz, C. E.; Scheidt, W. R. *Inorg. Chem.* **2007**, 46, 2286.
- (5) Sheldrick, G. M. *Acta Chrystallogr.* **1990**, A46, 467.
- (6) Sheldrick, G. M.: Program for the Refinement of Crystal Structures. Universität Göttingen, Germany, 1997.
- (7)  $R_1 = \sum \|F_o| - |F_c\| / \sum |F_o|$  and  $wR_2 = \left\{ \sum [w(F_o^2 - F_c^2)^2] / \sum [wF_o^4] \right\}^{1/2}$ . The conventional  $R$ -factors  $R_1$  are based on  $F$ , with  $F$  set to zero for negative  $F^2$ . The criterion of  $F^2 > 2\sigma(F^2)$  was used only for calculating  $R_1$ .  $R$ -factors based on  $F^2$  ( $wR_2$ ) are statistically about twice as large as those based on  $F$ , and  $R$ -factors based on ALL data will be even larger.
- (8) Sheldrick, G. M.: Program for empirical Absorption Correction of Area Detector Data. Universität Göttingen, Germany, 1996.
- (9) Sutter, T. P. G.; Hambright, P.; Thorpe, A. N.; Quoc, N. *Inorg. Chim. Acta* **1992**, 195, 131.
- (10) Earnshaw, A. *Introduction to Magnetochemistry*; Academic: London, 1968; Chapter 1.
- (11) Jaguar, version 7.0; Schrodinger, LLC, New York, NY, 2007.
- (12) (a) Becke, A. D. *Phys. Rev. A* **1988**, 38, 3098. (b) Becke, A. D. *J. Chem. Phys.* **1993**, 98, 5648.
- (13) (a) Hay, P. J.; Wadt, W. R. *J. Chem. Phys.* **1985**, 82, 270. (b) Wadt, W. R.; Hay, P. J. *J. Chem. Phys.* **1985**, 82, 284. (c) Hay, P. J.; Wadt, W. R. *J. Chem. Phys.* **1985**, 82, 299.
- (14) (a) Reiher, M.; Salomon, O.; Hess, B. A. *Theor. Chem. Acta* **2001**, 107, 48. (b) Salomon, O.; Reiher, M; Hess, B. A. *J. Chem. Phys.* **2002**, 117, 4729.
- (15) Dunning, T. H. *J. Chem. Phys.* **1989**, 90, 1007.

**Table S1.** Complete Crystallographic Details for [K(222)][Fe(TPP)(CN)] at 100, 296, 325 and 400K.

|   | [K(222)][Fe(TPP)(CN)]  | [K(222)][Fe(TPP)(CN)]  | [K(222)][Fe(TPP)(CN)]  | [K(222)][Fe(TPP)(CN)]  |
|---|--|--|--|--|
| chemical formula                        | C <sub>63</sub> H <sub>64</sub> FeKN <sub>7</sub> O <sub>6</sub> | C <sub>63</sub> H <sub>64</sub> FeKN <sub>7</sub> O <sub>6</sub> | C <sub>63</sub> H <sub>64</sub> FeKN <sub>7</sub> O <sub>6</sub> | C <sub>63</sub> H <sub>64</sub> FeKN <sub>7</sub> O <sub>6</sub> |
| FW                                      | 1110.16  | 1110.16  | 1110.16  | 1110.16  |
| <i>a</i> , Å                            | 14.0985(2)   | 14.2821(2)   | 14.3256(2)   | 14.3982(3)   |
| <i>b</i> , Å                            | 20.5735(3)   | 20.6984(3)   | 20.7453(3)   | 20.7783(4)   |
| <i>c</i> , Å                            | 20.3376(3)   | 20.5563(3)   | 20.5957(4)   | 20.6637(5)   |
| $\alpha$ , deg                          | 90.00  | 90.00  | 90.00  | 90.00  |
| $\beta$ , deg                           | 104.255(1)   | 104.453(1)   | 104.448(1)   | 104.417(1)   |
| $\gamma$ , deg                          | 90.00  | 90.00  | 90.00  | 90.00  |
| <i>V</i> , Å <sup>3</sup>               | 5717.40(14)  | 5884.47(15)  | 5927.24(17)  | 5987.3(2)  |
| space group                             | Cc   | Cc   | Cc   | Cc   |
| <i>Z</i>                                | 4  | 4  | 4  | 4  |
| temp, K                                 | 100  | 296  | 325  | 400  |
| D <sub>calcd</sub> , g cm <sup>-3</sup> | 1.290  | 1.253  | 1.244  | 1.232  |
| $\mu$ , mm <sup>-1</sup>                | 0.394  | 0.383  | 0.380  | 0.377  |
| final <i>R</i> indices                  | <i>R</i> <sub>1</sub> = 0.0301                                   | <i>R</i> <sub>1</sub> = 0.0325                                   | <i>R</i> <sub>1</sub> = 0.0389                                   | <i>R</i> <sub>1</sub> = 0.0285                                   |
| [I > 2 $\sigma$ (I)]                    | w <i>R</i> <sub>2</sub> = 0.0782                                 | w <i>R</i> <sub>2</sub> = 0.0804                                 | w <i>R</i> <sub>2</sub> = 0.0928                                 | w <i>R</i> <sub>2</sub> = 0.0739                                 |
| final <i>R</i> indices<br>(all data)    | <i>R</i> <sub>1</sub> = 0.0381                                   | <i>R</i> <sub>1</sub> = 0.0412                                   | <i>R</i> <sub>1</sub> = 0.0577                                   | <i>R</i> <sub>1</sub> = 0.0337                                   |
|   | w <i>R</i> <sub>2</sub> = 0.0793                                 | w <i>R</i> <sub>2</sub> = 0.0849                                 | w <i>R</i> <sub>2</sub> = 0.1014                                 | w <i>R</i> <sub>2</sub> = 0.0769                                 |

**Table S2.** Selected Structural Parameters for  $[\text{K}(222)\text{II}\text{Fe}(\text{TPP})(\text{CN})]$  at 100, 296, 325 and 400 K.<sup>a</sup>

| Complex  | $\Delta^b$ | $\Delta N_4^c$ | $(\text{Fe}-\text{N}_p)_{av}$ | Fe-C       | C-N        | Fe-C-N     | $\tau^d$ | ref. |
|--|------------|----------------|-------------------------------|------------|------------|------------|----------|------|
| Five-coordinate Porphyrinates                                      |            |                |                               |            |            |            |          |      |
| $[\text{K}(222)\text{II}\text{Fe}(\text{TPP})(\text{CN})]$ (100 K) | 0.23       | 0.17           | 1.986(7)                      | 1.8783(10) | 1.1662(14) | 177.19(10) | 6.3      | tw   |
| $[\text{K}(222)\text{II}\text{Fe}(\text{TPP})(\text{CN})]$ (296 K) | 0.42       | 0.35           | 2.047(8)                      | 2.028(3)   | 1.153(4)   | 175.7(2)   | 6.9      | tw   |
| $[\text{K}(222)\text{II}\text{Fe}(\text{TPP})(\text{CN})]$ (325 K) | 0.47       | 0.39           | 2.064(8)                      | 2.103(3)   | 1.134(3)   | 175.8(2)   | 7.2      | tw   |
| $[\text{K}(222)\text{II}\text{Fe}(\text{TPP})(\text{CN})]$ (400 K) | 0.54       | 0.45           | 2.089(8)                      | 2.108(3)   | 1.122(3)   | 175.8(2)   | 7.4      | tw   |

<sup>a</sup> Distance values in Å, Angle values in deg., tw = this work. <sup>b</sup> Displacement of iron atom from the 24-atom mean plane.

the positive numbers indicate a displacement toward the C–N. <sup>c</sup> Displacement of iron atom from the mean plane of the four pyrrole nitrogen atoms, the positive numbers indicate a displacement toward the C–N. <sup>d</sup> The angle of Fe–C vector tilted from the normal to the 24-atom mean plane.

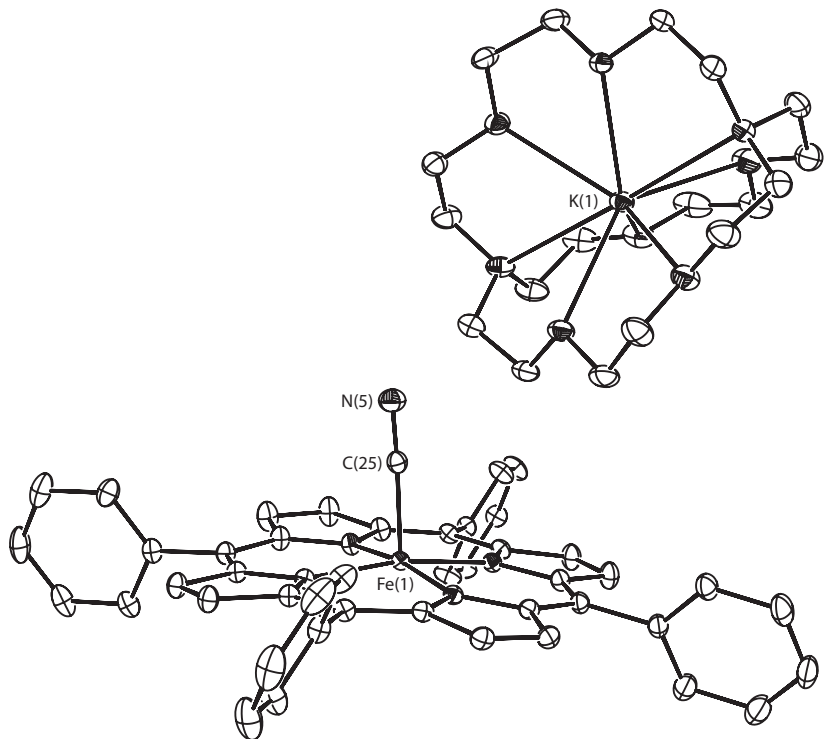


**Figure S1.** ORTEP diagram of asymmetric unit of  $[K(222)][Fe(TPP)(CN)]$  (100 K) displaying the atom labeling scheme. Thermal ellipsoids of all atoms are contoured at the 50% probability level. Hydrogen atoms have been omitted for clarity.

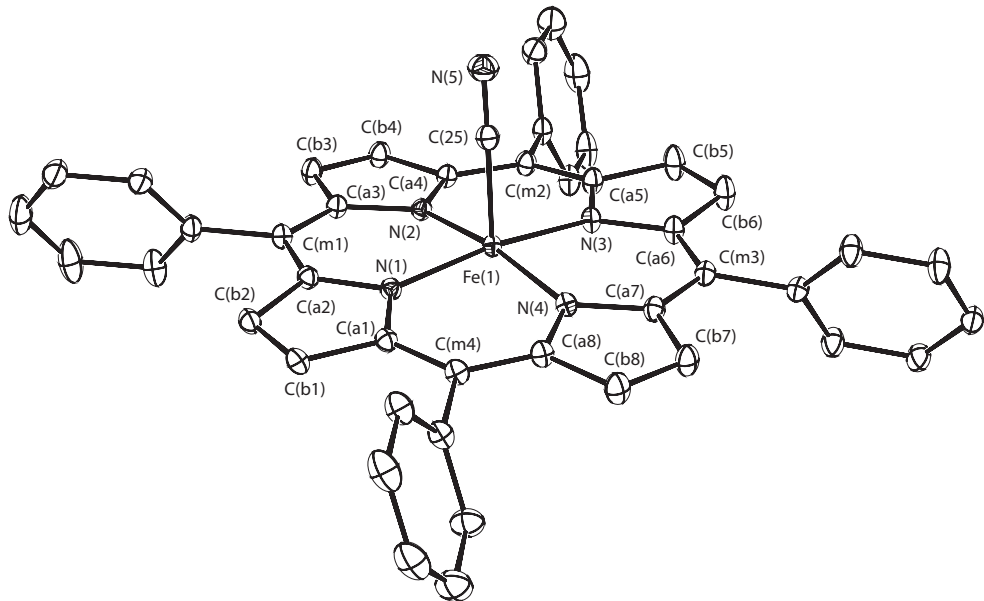


**Figure S2.** ORTEP diagram of the  $[Fe(TPP)(CN)]^-$  anion in  $[K(222)][Fe(TPP)(CN)]$  (100 K) displaying the atom labeling scheme. Thermal ellipsoids of all atoms are contoured at the 50% probability level. Hydrogen atoms have been omitted for clarity.

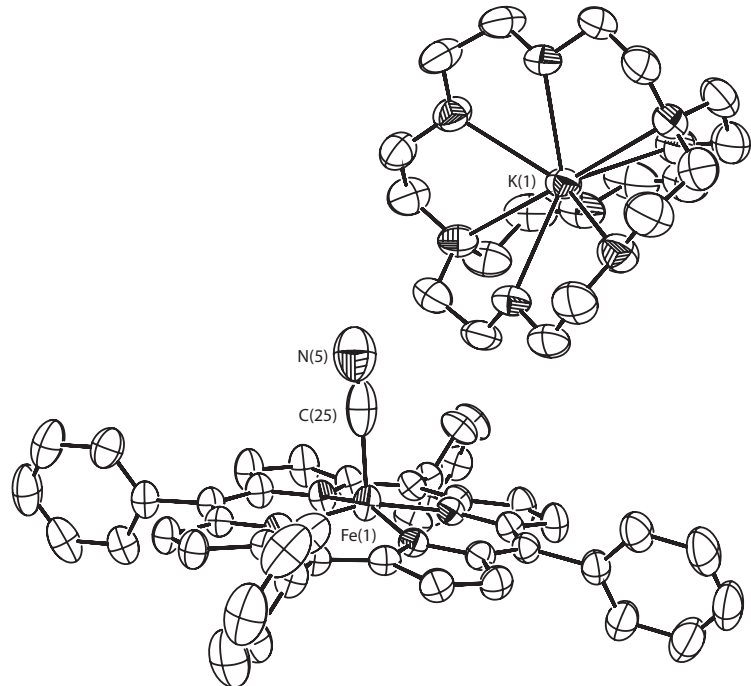


**Figure S3.** ORTEP diagram of asymmetric unit of  $[K(222)][Fe(TPP)(CN)]$  (296 K) displaying the atom labeling scheme. Thermal ellipsoids of all atoms are contoured at the 50% probability level. Hydrogen atoms have been omitted for clarity.

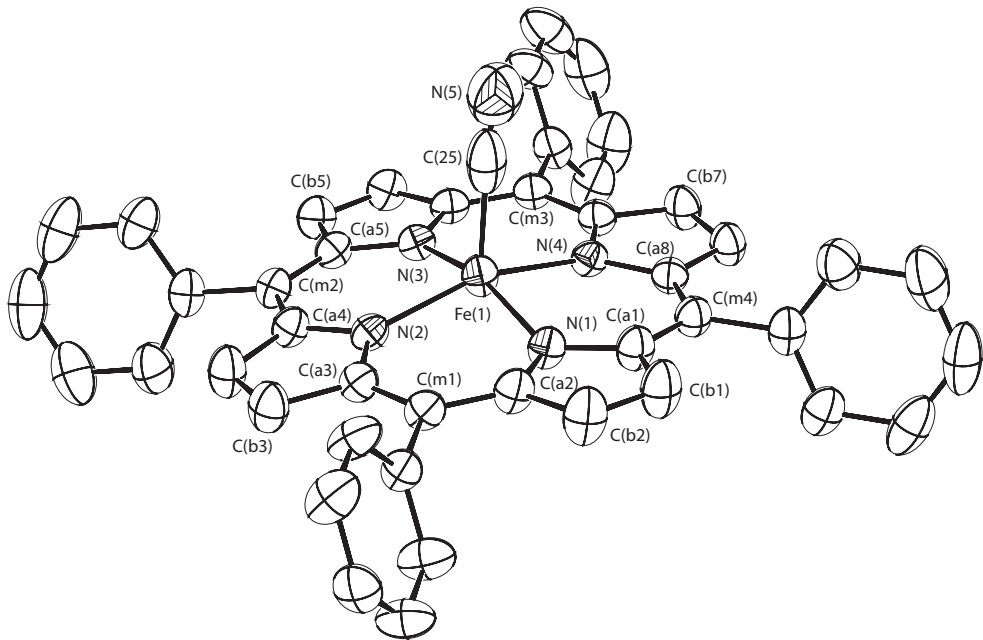


**Figure S4.** ORTEP diagram of the  $[Fe(TPP)(CN)]^-$  anion in  $[K(222)][Fe(TPP)(CN)]$  (296 K) displaying the atom labeling scheme. Thermal ellipsoids of all atoms are contoured at the 50% probability level. Hydrogen atoms have been omitted for clarity.

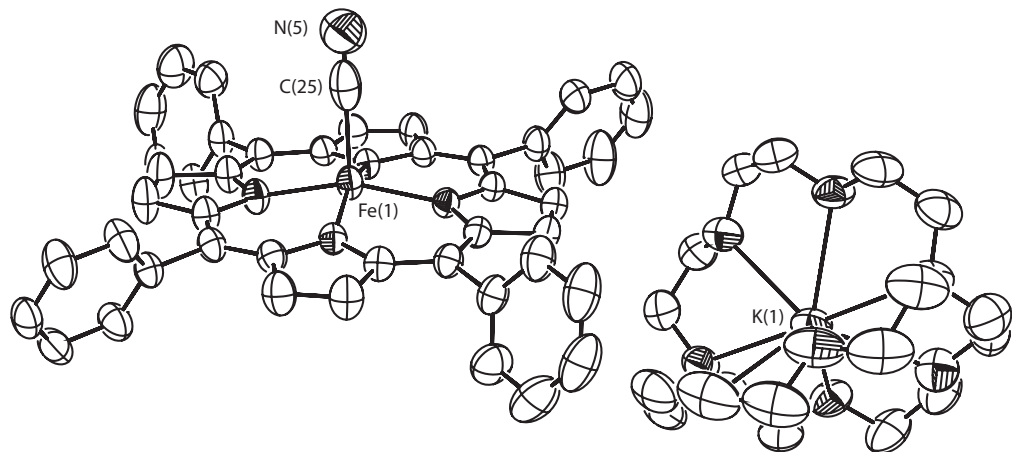


**Figure S5.** ORTEP diagram of asymmetric unit of  $[K(222)][Fe(TPP)(CN)]$  (325 K) displaying the atom labeling scheme. Thermal ellipsoids of all atoms are contoured at the 50% probability level. Hydrogen atoms have been omitted for clarity.

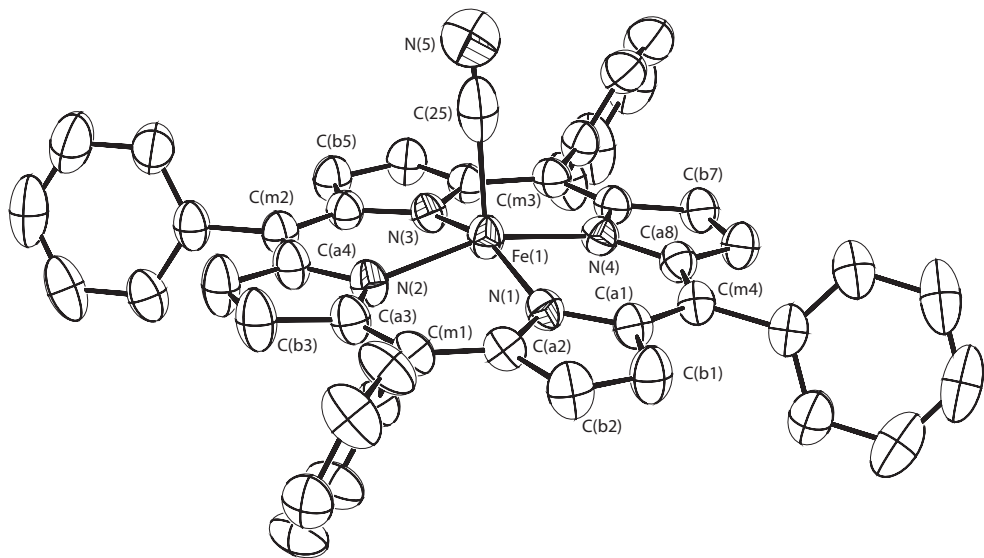


**Figure S6.** ORTEP diagram of the  $[Fe(TPP)(CN)]^-$  anion in  $[K(222)][Fe(TPP)(CN)]$  (325 K) displaying the atom labeling scheme. Thermal ellipsoids of all atoms are contoured at the 50% probability level. Hydrogen atoms have been omitted for clarity.

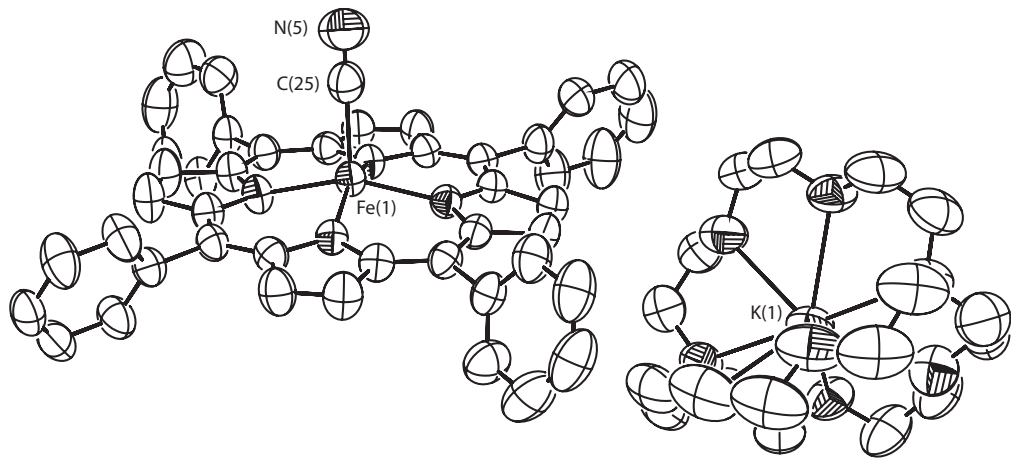


**Figure S7.** ORTEP diagram of asymmetric unit of  $[K(222)][Fe(TPP)(CN)]$  (400 K) displaying the atom labeling scheme. Thermal ellipsoids of all atoms are contoured at the 50% probability level. Hydrogen atoms have been omitted for clarity.

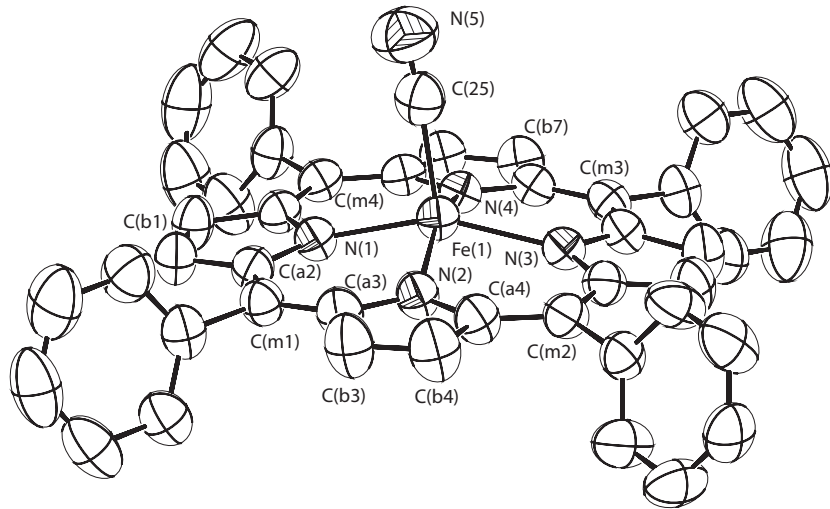


**Figure S8.** ORTEP diagram of the  $[Fe(TPP)(CN)]^-$  anion in  $[K(222)][Fe(TPP)(CN)]$  (400 K) displaying the atom labeling scheme. Thermal ellipsoids of all atoms are contoured at the 50% probability level. Hydrogen atoms have been omitted for clarity.

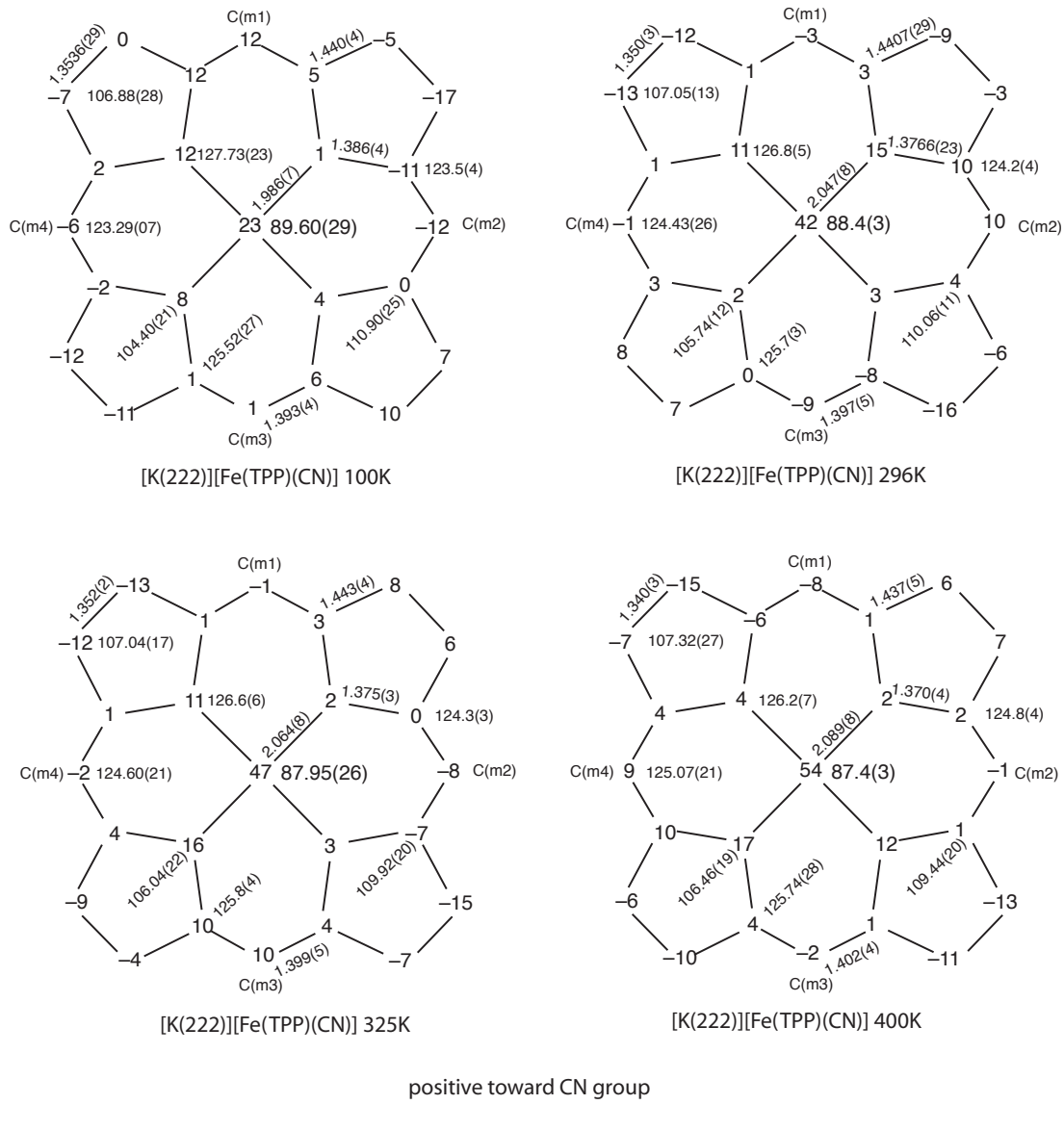


**Figure S9.** Formal diagram of the porphyrin cores of  $[K(222)][Fe(TPP)(CN)]$  structures at four different temperatures. Averaged values of the chemically unique bond distances (in Å) and angles (in degrees) are shown. The numbers in parentheses are the esd's calculated on the assumption that the averaged values were all drawn from the same population. The perpendicular displacements (in units of 0.01 Å) of the porphyrin core atoms from the 24-atom mean plane are also displayed. The positive values are towards the cyanide ligand positions.

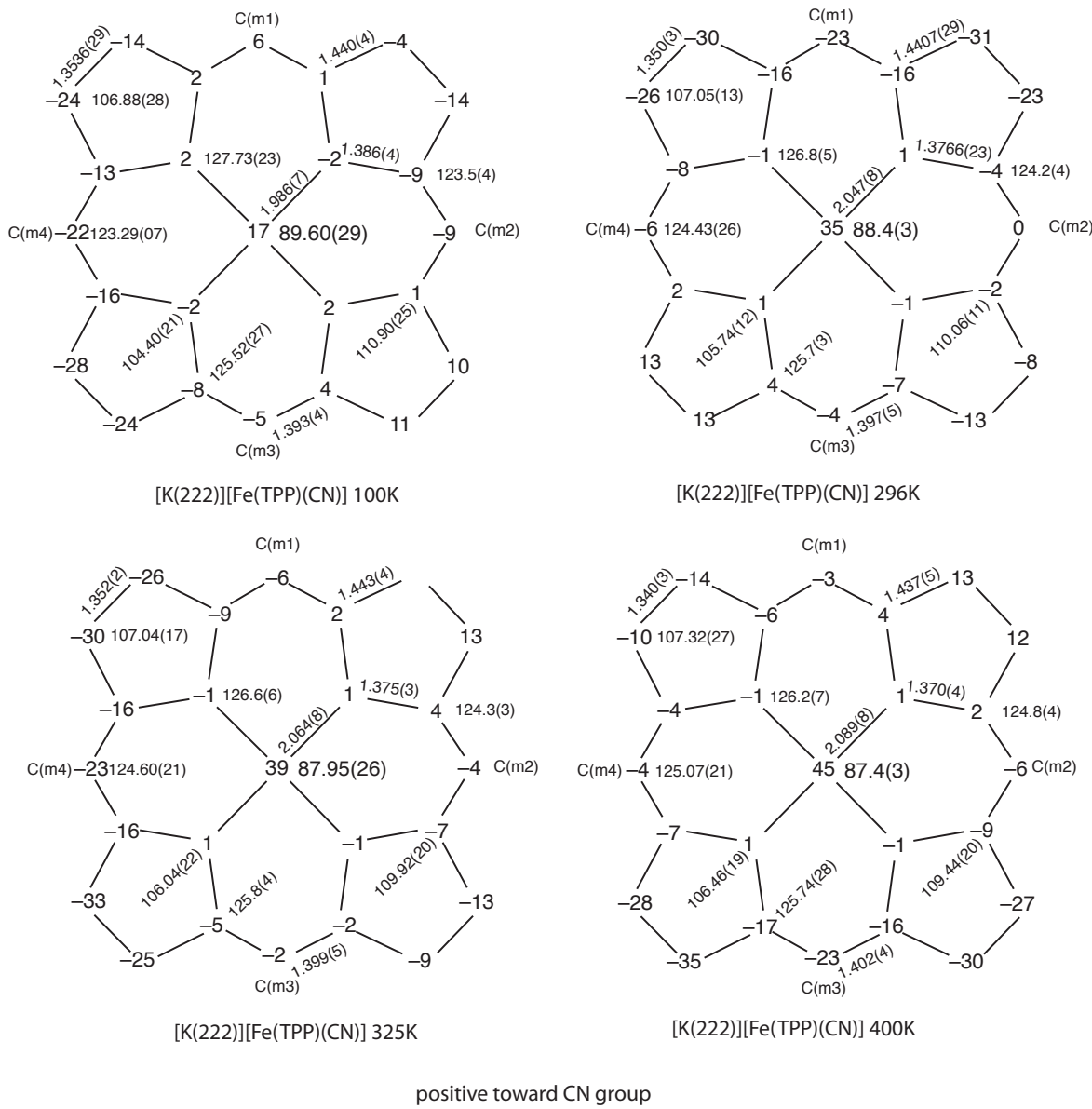


**Figure S10.** Formal diagram of the porphyrin cores of [K(222)][Fe(TPP)(CN)] structures at four different temperatures. Averaged values of the chemically unique bond distances (in Å) and angles (in degrees) are shown. The numbers in parentheses are the esd's calculated on the assumption that the averaged values were all drawn from the same population. The perpendicular displacements (in units of 0.01 Å) of the porphyrin core atoms from the 4-atom mean plane are also displayed. The positive values are towards the cyanide ligand positions.

**Table S3** Mössbauer Parameters of [K(222)][Fe(TPP)(CN)]

| T (K) | $\Delta E_Q$ (mm/s) | $\delta$ (mm/s) | $\Gamma$ (mm/s) |
|-------|---------------------|-----------------|-----------------|
| 25    | 1.83                | 0.37            | 0.38, 0.36      |
| 100   | 1.83                | 0.36            | 0.33, 0.33      |
| 200   | 1.82                | 0.35            | 0.32, 0.32      |
| 210   | 1.77                | 0.29            | 0.40, 0.33      |
| 220   | 1.70                | 0.30            | 0.47, 0.37      |
| 230   | 1.64                | 0.28            | 0.54, 0.37      |
| 240   | 1.53                | 0.28            | 0.60, 0.38      |
| 250   | 1.43                | 0.29            | 0.61, 0.35      |
| 260   | 1.43                | 0.30            | 0.62, 0.35      |
| 270   | 1.31                | 0.31            | 0.63, 0.35      |
| 280   | 1.20                | 0.35            | 0.59, 0.31      |
| 290   | 1.12                | 0.38            | 0.54, 0.30      |
| 295   | 0.87                | 0.48            | 0.41, 0.28      |
| 300   | 0.85                | 0.47            | 0.43, 0.27      |

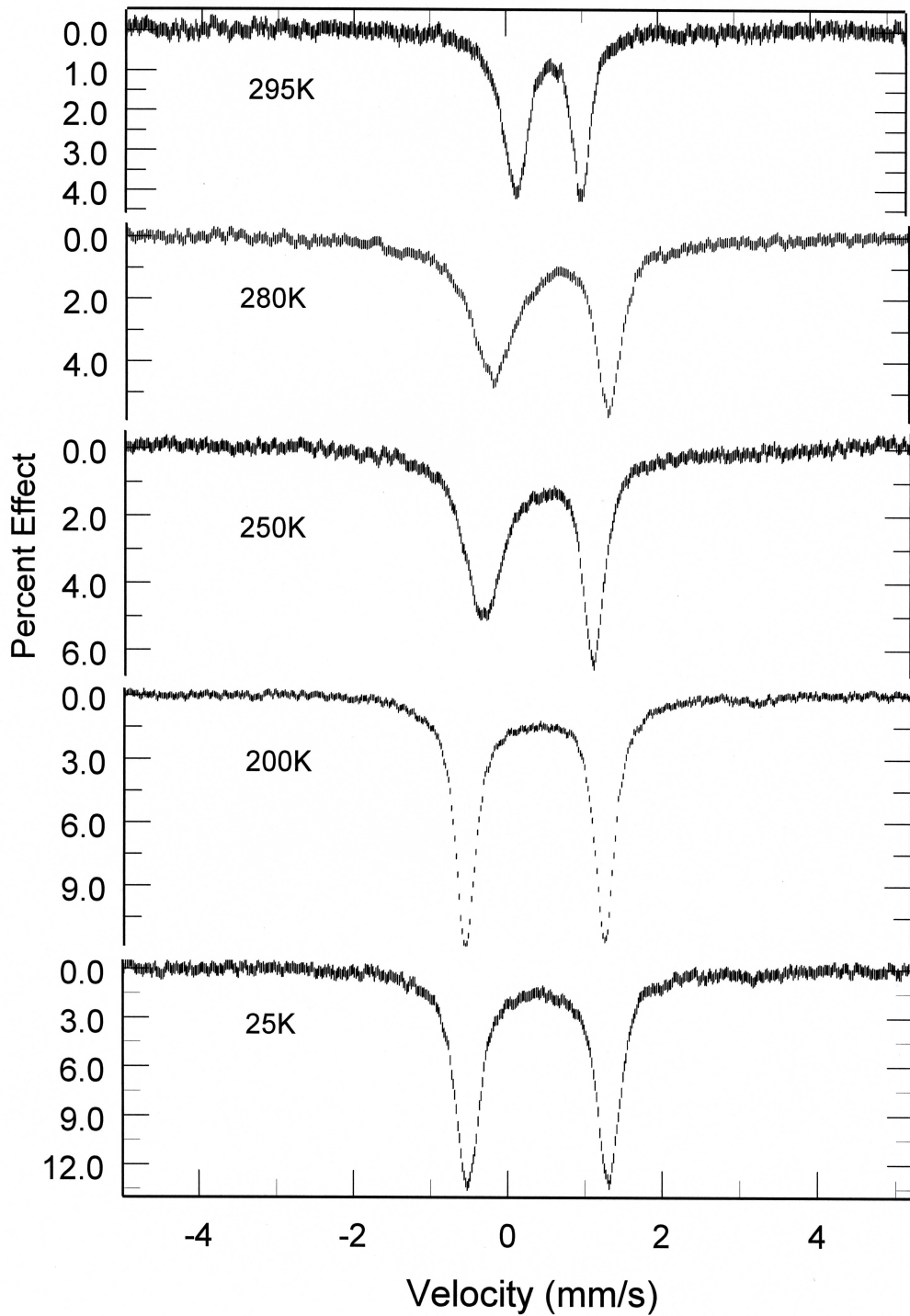


**Figure S11.** Selected Mössbauer spectra of  $[K(222)][Fe(\text{TPP})(\text{CN})]$  in 500mT field ( complete data are given in Table S3. ).

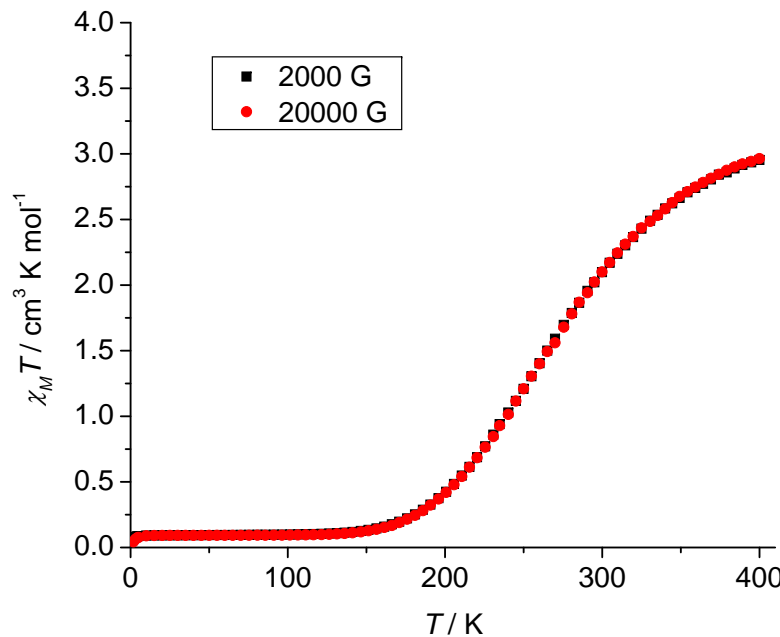


**Figure S12.** Temperature dependence of  $\chi_M T$  for  $[\text{K}(222)][\text{Fe}(\text{TPP})(\text{CN})]$  at two different magnetic field of 2000 and 20000 Gauss.

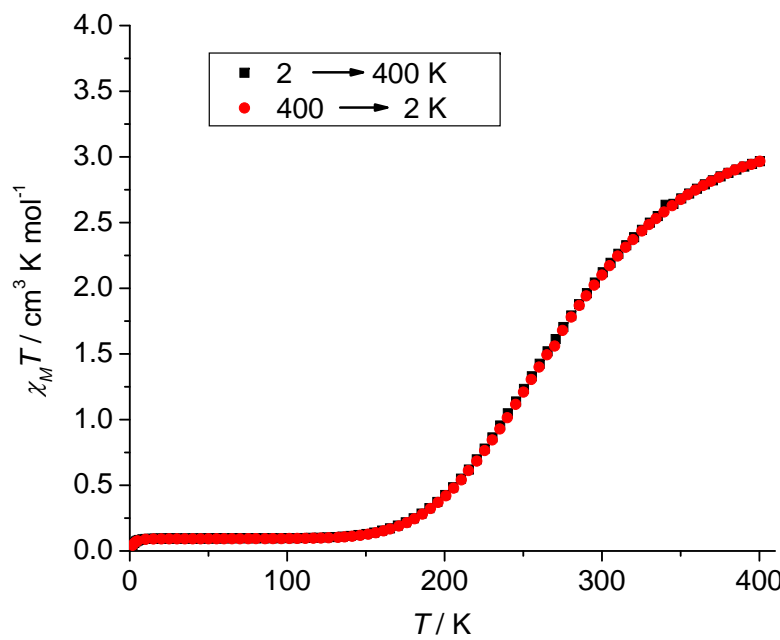


**Figure S13.**  $\chi_M T$  vs.  $T$  plot for  $[\text{K}(222)][\text{Fe}(\text{TPP})(\text{CN})]$  with temperature decreasing ( $400 \rightarrow 2 \text{ K}$ ) and increasing ( $2 \rightarrow 400 \text{ K}$ ) at magnetic field of 20000 Gauss.

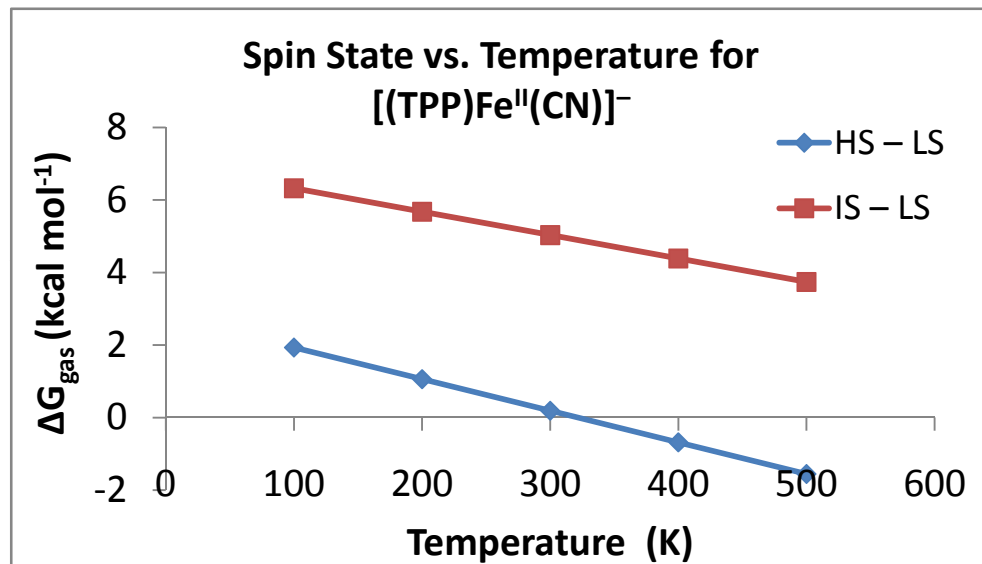


**Figure S14.** Spin state energetics as a function of temperature, referenced to the LS state. This temperature dependence is explicitly due to the gas-phase entropy,  $S(\text{gas})$ . At no point does the IS state become thermodynamically favored over both the LS and HS states.

|  | Fe-CN | C-N   | Fe-N <sub>p</sub> (avg) | N <sub>p</sub> -Fe-CN (avg) | N <sub>p</sub> -Fe-N <sub>p</sub> (avg) |
|--|-------|-------|-------------------------|-----------------------------|---|
| <b>low spin, <math>S = 0</math></b>          | 1.873 | 1.172 | 2.012                   | 94.4                        | 171.2                                   |
| <b>intermediate spin, <math>S = 1</math></b> | 2.123 | 1.173 | 2.015, 2.056            | 95.0, 98.7                  | 170.0, 162.6                            |
| <b>high spin, <math>S = 2</math></b>         | 2.100 | 1.172 | 2.126                   | 103.2                       | 153.6                                   |
| <b>crystal (100 K)</b>                       | 1.878 | 1.166 | 1.986                   | 94.82                       | 170.36                                  |
| <b>crystal (296 K)</b>                       | 2.028 | 1.153 | 2.047                   | 99.73                       | 160.52                                  |
| <b>crystal (325 K)</b>                       | 2.103 | 1.134 | 2.064                   | 100.82                      | 158.21                                  |
| <b>crystal (400 K)</b>                       | 2.108 | 1.122 | 2.089                   | 102.4                       | 155.16                                  |

All bond lengths listed in Å and bond angles listed in degrees.

The structural parameters predicted by DFT support the conclusion that the  $S = 1$  state is not accessible experimentally, as the large anisotropy in Fe-N bond lengths and Fe-centered angles are not observed in the temperature-dependent crystal determinations.

**Table S4.** Calculated and crystallographic structural parameters for the three spin-states.

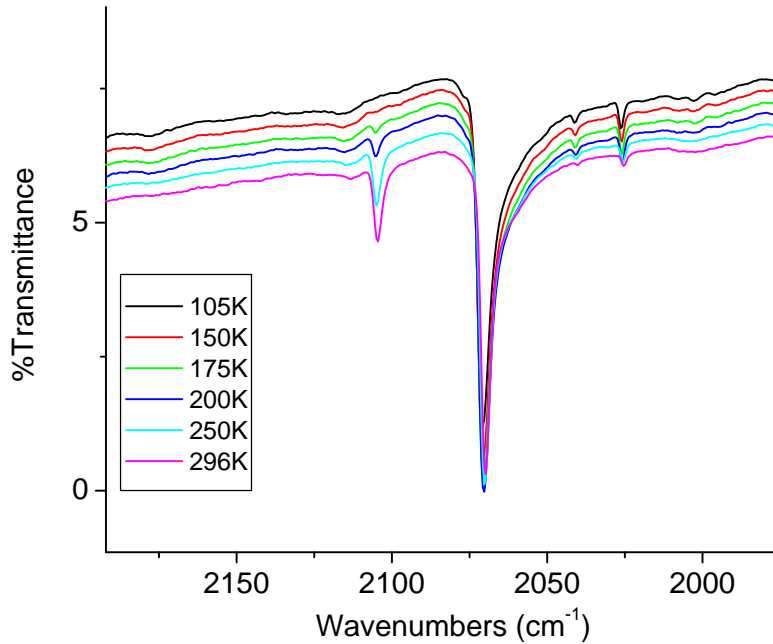


**Figure S15.** Multi-temperature (cooling from 296 to 105 K) measured IR spectra. Only C≡N stretches are showed for clarity.  $\nu_{C\equiv N}$  at 2070 and 2105 cm<sup>-1</sup> are correlated to LS and HS states respectively ( $\nu_{C\equiv N}$  at 2025 and 2040 cm<sup>-1</sup> are correlated to isotopic stretches of  $^{13}\text{C}\equiv ^{14}\text{N}$  and  $^{12}\text{C}\equiv ^{15}\text{N}$  ).

**Table S5.** Optimized Cartesian coordinates for the low-, intermediate-, and high-spin structures.

|   |  |              |              |              |
|---|--|--------------|--------------|--------------|
|   | C  | 2.544510799  | -6.428649063 | 1.685037279  |
|   | H  | 3.079836534  | -7.116084298 | 1.035022640  |
|   | C  | 2.312488079  | -6.764069510 | 3.020345963  |
|   | H  | 2.661126669  | -7.714374060 | 3.415666733  |
| low-spin ( $S = 0$ ) (TPP)Fe <sup>II</sup> (CN) | C  | 1.629438222  | -5.866719147 | 3.842848061  |
|   | H  | 1.440060423  | -6.117116192 | 4.883708590  |
|   | C  | 1.182316457  | -4.646482900 | 3.334074559  |
|   | H  | 0.649152399  | -3.951337437 | 3.976281193  |
|   | C  | -3.396814581 | -2.380331919 | -2.694052028 |
|   | C  | -3.198861317 | -2.471740112 | -4.080869981 |
|   | H  | -2.315451577 | -2.014019836 | -4.514813633 |
|   | C  | -4.112524459 | -3.144229102 | -4.892389781 |
|   | H  | -3.937030196 | -3.206656052 | -5.963345971 |
|   | C  | -5.244406060 | -3.739058683 | -4.332607345 |
|   | H  | -5.956608037 | -4.263349818 | -4.964584408 |
|   | C  | -5.454253395 | -3.655659182 | -2.955438455 |
|   | H  | -6.334495950 | -4.112297129 | -2.510018565 |
|   | C  | -4.538653302 | -2.982908672 | -2.145070520 |
|   | H  | -4.705487978 | -2.915170556 | -1.074007067 |
|   | C  | 1.292455836  | -0.258809631 | -1.415647906 |
| =====   | =====  | =====        | =====        | =====        |
|   | intermediate-spin ( $S = 1$ ) (TPP)Fe <sup>II</sup> (CN) |              |              |              |
|   | =====  | =====        | =====        | =====        |
| Fe  | 0.063329569  | -0.025549238 | -0.092665646 |              |
| N   | -1.427213757   | 0.551618423  | -1.314680174 |              |
| N   | -0.720834336   | -1.927346578 | -0.062531555 |              |
| N   | 1.323826620  | -0.558683437 | 1.390157640  |              |
| N   | 0.434790230  | 1.950440972  | 0.334361259  |              |
| N   | 2.260272129  | -0.458741384 | -2.510470192 |              |
| C   | -1.736517420   | 1.832511544  | -1.709427648 |              |
| C   | -2.297788044   | -0.271609365 | -1.987677399 |              |
| C   | -1.672217082   | -2.418677078 | -0.917620549 |              |
| C   | -0.196073669   | -3.013810323 | 0.588777014  |              |
| C   | 1.576711249  | -1.829955840 | 1.846005712  |              |
| C   | 2.251521328  | 0.250264059  | 2.000253483  |              |
| C   | 1.477373544  | 2.419591558  | 1.090072128  |              |
| C   | -0.106105795   | 3.043750935  | -0.290822163 |              |
| C   | -2.835888746   | 1.811957348  | -2.654053958 |              |
| H   | -3.291467263   | 2.684511723  | -3.098913111 |              |
| C   | -3.176564525   | 0.512355382  | -2.832194623 |              |
| H   | -3.9666927951  | 0.111049551  | -3.449777086 |              |
| C   | -1.777794227   | -3.851335356 | -0.774384762 |              |
| H   | -2.444354937   | -4.490454750 | -1.334612883 |              |
| C   | -0.872522334   | -4.218006512 | 0.172981671  |              |
| H   | -0.664522546   | -5.211313531 | 0.542568502  |              |
| C   | 2.710260800  | -1.822661790 | 2.748948515  |              |
| H   | 3.125035066  | -2.694352091 | 3.232633812  |              |
| C   | 3.131660778  | -0.538044646 | 2.839116670  |              |
| H   | 3.960011610  | -0.148269970 | 3.412567920  |              |
| C   | 1.570785107  | 3.854297365  | 0.973843499  |              |
| H   | 2.297674232  | 4.477143361  | 1.474742279  |              |
| C   | 0.590250098  | 4.242249012  | 0.114234437  |              |
| H   | 0.372785465  | 5.242421714  | -0.229323982 |              |
| C   | -2.403551820   | -1.660559199 | -1.846639961 |              |
| C   | 0.881217737  | -2.988787675 | 1.487844965  |              |
| C   | 2.354887382  | 1.636311159  | 1.855344961  |              |
| C   | -1.127447849   | 3.009035536  | -1.255554101 |              |
| C   | -1.558550832   | 4.307398806  | -1.862638594 |              |
| C   | -1.317445721   | 4.571729816  | -3.220957931 |              |
| H   | -0.813831069   | 3.818145411  | -3.819082934 |              |
| C   | -1.702768507   | 5.782105777  | -3.797479855 |              |
| H   | -1.499352801   | 5.964230620  | -4.849872341 |              |

**Table S5.** Continued.

|  |              |              |              |  |   |              |              |              |
|--|--------------|--------------|--------------|--|---|--------------|--------------|--------------|
| C  | -2.338587909 | 6.757739087  | -3.027155653 |  | C | -1.737164828 | -3.875421529 | -0.818544221 |
| H  | -2.638684116 | 7.701753286  | -3.475439480 |  | H | -2.423589930 | -4.512667402 | -1.356613076 |
| C  | -2.583351606 | 6.509791458  | -1.675383368 |  | C | -0.839304318 | -4.244895227 | 0.135027390  |
| H  | -3.080556328 | 7.261336823  | -1.066545705 |  | H | -0.665260785 | -5.237145700 | 0.524623832  |
| C  | -2.196954624 | 5.298248089  | -1.098900890 |  | C | 2.661108317  | -1.818102936 | 2.890527960  |
| H  | -2.392979375 | 5.107697314  | -0.047788674 |  | H | 3.071133607  | -2.678167656 | 3.400267784  |
| C  | 3.490431799  | 2.335046842  | 2.535732573  |  | C | 3.077101528  | -0.526170182 | 2.980794654  |
| C  | 4.568814803  | 2.820773348  | 1.779351816  |  | H | 3.885134305  | -0.135628143 | 3.582407766  |
| H  | 4.563222633  | 2.671947675  | 0.703480277  |  | C | 1.602213261  | 3.870987983  | 0.944042224  |
| C  | 5.636543764  | 3.473517485  | 2.394217080  |  | H | 2.299317933  | 4.502412937  | 1.475664796  |
| H  | 6.464614925  | 3.837606389  | 1.790673506  |  | C | 0.631290370  | 4.258809669  | 0.072775900  |
| C  | 5.645813487  | 3.653952960  | 3.778255946  |  | H | 0.405357891  | 5.262784440  | -0.254727759 |
| H  | 6.477956229  | 4.162983346  | 4.258102671  |  | C | -2.385724516 | -1.662674626 | -1.869736469 |
| C  | 4.579987625  | 3.175826201  | 4.541752999  |  | C | 0.892148211  | -3.003742973 | 1.508665772  |
| H  | 4.576999907  | 3.314031509  | 5.620210774  |  | C | 2.345576646  | 1.641639907  | 1.885304464  |
| C  | 3.512364040  | 2.522404308  | 3.924976724  |  | C | -1.110986556 | 3.019773744  | -1.293883462 |
| H  | 2.680981352  | 2.153147324  | 4.519170216  |  | C | -1.583601264 | 4.327281967  | -1.844258215 |
| C  | 1.348325718  | -4.293130947 | 2.059766117  |  | C | -1.434516903 | 4.622710099  | -3.209339330 |
| C  | 2.031548200  | -5.219772821 | 1.256027808  |  | H | -0.963132614 | 3.888933503  | -3.855961995 |
| H  | 2.216427824  | -4.973824041 | 0.214199439  |  | C | -1.869611718 | 5.840415620  | -3.731639471 |
| C  | 2.479319808  | -6.431947626 | 1.782313042  |  | H | -1.737977960 | 6.049554707  | -4.790616271 |
| H  | 3.011339606  | -7.131665323 | 1.142140020  |  | C | -2.464966658 | 6.788992932  | -2.898623952 |
| C  | 2.252798904  | -6.744033382 | 3.124440076  |  | H | -2.805136528 | 7.738216203  | -3.305385362 |
| H  | 2.602490352  | -7.688017142 | 3.534969171  |  | C | -2.620272894 | 6.509478781  | -1.539830941 |
| C  | 1.574597967  | -5.831356909 | 3.934222571  |  | H | -3.087739909 | 7.240112491  | -0.884086417 |
| H  | 1.390578355  | -6.063097103 | 4.980766556  |  | C | -2.183374956 | 5.291507456  | -1.017874991 |
| C  | 1.127542174  | -4.618904435 | 3.406076031  |  | H | -2.311983960 | 5.072668431  | 0.038138937  |
| H  | 0.599683765  | -3.910336077 | 4.038662921  |  | C | 3.448063732  | 2.356599640  | 2.603614592  |
| C  | -3.337471901 | -2.387957105 | -2.760730802 |  | C | 4.532107683  | 2.881670789  | 1.881248480  |
| C  | -3.066375689 | -2.451661578 | -4.136937626 |  | H | 4.557101425  | 2.747537263  | 0.803656790  |
| H  | -2.174475281 | -1.963790691 | -4.517151165 |  | C | 5.566117885  | 3.555489407  | 2.530644455  |
| C  | -3.913467386 | -3.141054187 | -5.003673986 |  | H | 6.398123845  | 3.949510333  | 1.952158077  |
| H  | -3.679093095 | -3.183616910 | -6.064341167 |  | C | 5.537279775  | 3.718721709  | 3.916831669  |
| C  | -5.051930382 | -3.781084344 | -4.512036729 |  | H | 6.342439033  | 4.245075104  | 4.423610341  |
| H  | -5.711692604 | -4.320898958 | -5.186954343 |  | C | 4.466664584  | 3.201785603  | 4.647174048  |
| C  | -5.335484061 | -3.723942120 | -3.147227473 |  | H | 4.431539890  | 3.328104907  | 5.726695071  |
| H  | -6.222013954 | -4.215461088 | -2.754710471 |  | C | 3.432864364  | 2.527671164  | 3.995836599  |
| C  | -4.486452819 | -3.034097653 | -2.281058831 |  | H | 2.596129175  | 2.133846376  | 4.565376976  |
| H  | -4.711087990 | -2.987984787 | -1.219464339 |  | C | 1.317182352  | -4.305476078 | 2.110862947  |
| C  | 1.486764211  | -0.297777531 | -1.643615299 |  | C | 1.949209291  | -5.284006105 | 1.326273219  |
| =====  |              |              |              |  |   |              |              |              |
| high-spin ( $S = 2$ ) (TPP)Fe <sup>II</sup> (CN) |              |              |              |  |   |              |              |              |
| =====  |              |              |              |  |   |              |              |              |
| Fe   | 0.276899607  | -0.061369316 | -0.301427035 |  | C | 2.350239102  | -6.498870010 | 1.882063112  |
| N  | -1.435910516 | 0.573609567  | -1.396143862 |  | H | 2.844203954  | -7.239113167 | 1.257309223  |
| N  | -0.634586867 | -1.971714340 | -0.143856598 |  | C | 2.126559549  | -6.761516852 | 3.234794197  |
| N  | 1.334611188  | -0.577478971 | 1.476924086  |  | H | 2.439494797  | -7.708193204 | 3.668370964  |
| N  | 0.512300839  | 1.969532103  | 0.246839638  |  | C | 1.499064688  | -5.798510145 | 4.026380556  |
| N  | 2.497617352  | -0.498131907 | -2.663882331 |  | H | 1.315208675  | -5.993865162 | 5.080227425  |
| C  | -1.762878284 | 1.852490227  | -1.747136670 |  | C | 1.098566930  | -4.584133446 | 3.468727399  |
| C  | -2.324236797 | -0.260528910 | -2.014972868 |  | H | 0.604904508  | -3.838852064 | 4.085168695  |
| C  | -1.610492441 | -2.439960556 | -0.982531745 |  | C | -3.373767146 | -2.386743407 | -2.731806856 |
| C  | -0.137745901 | -3.044173015 | 0.543283442  |  | C | -3.182864859 | -2.451538147 | -4.121474055 |
| C  | 1.564482044  | -1.841984593 | 1.939499693  |  | H | -2.309831608 | -1.971460727 | -4.553225099 |
| C  | 2.231688006  | 0.251517160  | 2.092271551  |  | C | -4.087514301 | -3.129468861 | -4.938701873 |
| C  | 1.523339416  | 2.426942672  | 1.047410166  |  | H | -3.915657683 | -3.173017459 | -6.011561442 |
| C  | -0.052921443 | 3.056419895  | -0.360281339 |  | C | -5.204227391 | -3.755419468 | -4.382310625 |
| C  | -2.914920091 | 1.831167099  | -2.630905420 |  | H | -5.909136704 | -4.285068841 | -5.018640100 |
| H  | -3.406318224 | 2.700401616  | -3.044338243 |  | C | -5.408572224 | -3.696413975 | -3.002885175 |
| C  | -3.256415217 | 0.525384917  | -2.803357769 |  | H | -6.278042344 | -4.176395382 | -2.560008093 |
| H  | -4.080988314 | 0.129360045  | -3.378909851 |  | C | -4.501702544 | -3.018988464 | -2.186895629 |
| C  |              |              |              |  |   |              |              |              |
| C  |              |              |              |  |   |              |              |              |
| C  |              |              |              |  |   |              |              |              |

**Table S6.** Unscaled frequencies for the optimized low-, intermediate-, and high-spin structures.

| low-spin ( $S = 0$ ) (TPP)Fe <sup>II</sup> (CN)          |         |         |         |         |         |  |         |         |
|--|---------|---------|---------|---------|---------|--|---------|---------|
| 15.07  | 23.44   | 32.96   | 35.39   | 37.28   | 39.96   | 939.86   | 940.33  | 989.89  |
| 42.55  | 44.77   | 50.89   | 55.81   | 56.08   | 60.78   | 999.77   | 1000.17 | 1000.67 |
| 72.36  | 73.43   | 86.15   | 96.75   | 118.07  | 124.26  | 1001.21  | 1003.74 | 1010.78 |
| 139.31   | 140.24  | 196.50  | 204.89  | 220.14  | 221.97  | 1018.09  | 1018.35 | 1019.10 |
| 227.52   | 236.47  | 240.93  | 245.93  | 246.93  | 251.37  | 1019.11  | 1022.43 | 1027.92 |
| 277.25   | 282.00  | 290.56  | 293.85  | 303.16  | 306.85  | 1031.76  | 1042.08 | 1045.50 |
| 317.02   | 317.94  | 336.92  | 371.83  | 398.11  | 405.80  | 1045.53  | 1059.86 | 1065.02 |
| 413.38   | 418.13  | 418.95  | 419.07  | 419.36  | 419.85  | 1067.12  | 1074.49 | 1101.57 |
| 420.26   | 449.54  | 463.45  | 467.11  | 473.08  | 474.12  | 1102.52  | 1103.24 | 1103.96 |
| 513.85   | 539.67  | 540.85  | 562.62  | 564.34  | 571.50  | 1104.77  | 1107.95 | 1108.68 |
| 574.63   | 585.35  | 633.88  | 634.36  | 634.54  | 635.95  | 1115.79  | 1118.09 | 1118.19 |
| 651.34   | 677.00  | 678.00  | 678.71  | 683.06  | 684.17  | 1183.79  | 1184.06 | 1205.50 |
| 687.41   | 693.81  | 718.50  | 718.78  | 719.32  | 719.57  | 1205.85  | 1205.98 | 1206.24 |
| 730.95   | 740.23  | 742.44  | 754.67  | 761.14  | 767.58  | 1206.96  | 1233.05 | 1240.39 |
| 775.50   | 776.71  | 790.49  | 803.30  | 803.60  | 809.93  | 1259.89  | 1264.74 | 1278.95 |
| 839.24   | 847.11  | 849.51  | 859.66  | 861.51  | 861.72  | 1280.26  | 1303.18 | 1322.75 |
| 862.00   | 862.41  | 882.76  | 891.36  | 893.84  | 899.70  | 1324.91  | 1327.31 | 1328.82 |
| 908.18   | 909.02  | 909.57  | 911.75  | 935.60  | 937.77  | 1340.85  | 1342.48 | 1344.70 |
| 937.88   | 938.08  | 988.47  | 988.52  | 988.94  | 989.27  | 1358.43  | 1358.67 | 1359.94 |
| 998.33   | 998.65  | 998.73  | 999.05  | 1003.46 | 1008.75 | 1360.48  | 1374.63 | 1378.22 |
| 1015.07  | 1016.36 | 1018.76 | 1018.98 | 1019.15 | 1019.54 | 1378.90  | 1388.72 | 1403.26 |
| 1025.88  | 1042.18 | 1043.60 | 1045.26 | 1059.31 | 1064.56 | 1479.53  | 1480.30 | 1481.16 |
| 1065.43  | 1073.58 | 1101.99 | 1102.38 | 1102.47 | 1102.97 | 1481.94  | 1483.74 | 1491.17 |
| 1105.24  | 1105.78 | 1107.52 | 1114.68 | 1182.29 | 1182.94 | 1497.27  | 1517.20 | 1533.38 |
| 1183.06  | 1183.19 | 1204.27 | 1204.89 | 1205.08 | 1205.69 | 1535.09  | 1537.27 | 1539.50 |
| 1207.76  | 1236.55 | 1238.53 | 1260.34 | 1270.01 | 1270.14 | 1554.29  | 1562.62 | 1565.42 |
| 1271.63  | 1298.62 | 1322.92 | 1326.58 | 1327.10 | 1328.37 | 1568.85  | 1590.04 | 1601.11 |
| 1341.07  | 1342.35 | 1343.76 | 1358.30 | 1358.71 | 1358.95 | 1605.77  | 1618.16 | 1628.90 |
| 1358.97  | 1376.31 | 1381.14 | 1382.56 | 1389.56 | 1404.75 | 1629.85  | 1631.76 | 1632.82 |
| 1480.50  | 1481.05 | 1481.14 | 1481.30 | 1493.69 | 1495.91 | 1654.27  | 1655.99 | 1657.76 |
| 1504.37  | 1521.31 | 1535.13 | 1535.57 | 1538.72 | 1541.50 | 1658.58  | 2213.14 | 3164.48 |
| 1556.74  | 1571.75 | 1573.07 | 1575.01 | 1601.44 | 1602.23 | 3164.76  | 3165.45 | 3166.54 |
| 1612.74  | 1621.20 | 1630.25 | 1631.31 | 1631.39 | 1632.41 | 3178.69  | 3188.02 | 3188.57 |
| 1656.57  | 1657.00 | 1657.16 | 1657.88 | 2214.12 | 3167.39 | 3189.14  | 3190.18 | 3196.23 |
| 3167.57  | 3167.62 | 3168.10 | 3177.91 | 3178.41 | 3178.49 | 3197.77  | 3200.40 | 3201.17 |
| 3178.76  | 3191.02 | 3191.43 | 3191.83 | 3192.02 | 3200.38 | 3203.24  | 3204.94 | 3205.88 |
| 3200.95  | 3201.29 | 3203.51 | 3206.93 | 3208.33 | 3208.76 | 3208.76  | 3210.85 | 3225.26 |
| 3210.28  | 3257.58 | 3258.85 | 3260.01 | 3261.44 | 3277.68 | 3257.73  | 3258.27 | 3258.82 |
| 3278.89  | 3280.12 | 3281.60 |         |         |         | 3277.81  | 3278.38 | 3279.40 |
| intermediate-spin ( $S = 1$ ) (TPP)Fe <sup>II</sup> (CN) |         |         |         |         |         |  |         |         |
| 14.67  | 26.02   | 26.74   | 33.74   | 34.65   | 35.25   | high-spin ( $S = 2$ ) (TPP)Fe <sup>II</sup> (CN) |         |         |
| 40.21  | 45.40   | 52.07   | 54.42   | 56.71   | 59.35   | 17.50  | 26.66   | 28.12   |
| 61.65  | 67.71   | 87.42   | 98.48   | 106.49  | 122.23  | 30.67  | 31.39   | 39.21   |
| 138.22   | 141.88  | 194.17  | 194.39  | 200.07  | 211.85  | 43.29  | 49.27   | 52.76   |
| 214.72   | 221.34  | 222.93  | 235.97  | 241.18  | 243.04  | 55.40  | 56.77   | 56.91   |
| 250.96   | 263.67  | 266.60  | 281.34  | 292.05  | 293.31  | 60.30  | 75.43   | 85.64   |
| 300.19   | 317.13  | 319.20  | 320.01  | 337.40  | 368.62  | 137.78   | 182.69  | 185.57  |
| 376.25   | 399.61  | 411.27  | 412.22  | 418.29  | 419.36  | 189.03   | 197.22  |         |
| 419.93   | 421.92  | 448.19  | 461.97  | 468.52  | 483.38  | 214.42   | 217.32  | 220.46  |
| 512.89   | 538.07  | 538.67  | 559.44  | 564.16  | 571.85  | 224.71   | 229.04  | 242.06  |
| 572.87   | 578.76  | 633.87  | 634.19  | 634.56  | 635.31  | 246.03   | 251.61  | 256.42  |
| 650.86   | 675.11  | 676.08  | 678.19  | 683.90  | 685.61  | 278.92   | 280.41  | 289.16  |
| 689.04   | 693.77  | 719.44  | 719.87  | 720.69  | 720.84  | 296.03   | 318.89  | 324.75  |
| 731.51   | 740.23  | 744.96  | 754.28  | 762.65  | 769.59  | 326.06   | 330.60  | 339.54  |
| 774.40   | 778.97  | 793.54  | 804.93  | 805.17  | 810.15  | 372.93   | 393.19  | 402.59  |
| 840.30   | 843.62  | 850.72  | 862.49  | 863.03  | 863.54  | 404.31   | 418.77  | 420.43  |
| 864.03   | 864.37  | 883.12  | 892.04  | 895.70  | 900.27  | 420.50   | 421.43  | 437.76  |
| 911.57   | 913.65  | 915.34  | 916.49  | 937.36  | 939.30  | 440.26   | 443.19  | 452.61  |
|  |         |         |         |         |         | 511.32   | 532.35  | 535.26  |
|  |         |         |         |         |         | 556.95   | 568.33  | 572.91  |
|  |         |         |         |         |         | 575.47   | 579.23  | 633.74  |
|  |         |         |         |         |         | 634.13   | 634.46  | 635.06  |
|  |         |         |         |         |         | 650.44   | 673.02  | 674.91  |
|  |         |         |         |         |         | 684.44   | 686.56  | 690.43  |
|  |         |         |         |         |         | 692.01   | 695.35  | 719.74  |
|  |         |         |         |         |         | 720.13   | 720.61  | 720.86  |
|  |         |         |         |         |         | 733.01   | 741.80  | 745.78  |
|  |         |         |         |         |         | 752.57   | 765.03  | 768.15  |
|  |         |         |         |         |         | 776.91   | 777.90  | 797.86  |
|  |         |         |         |         |         | 802.80   | 803.97  | 807.75  |
|  |         |         |         |         |         | 836.67   | 842.82  | 845.55  |
|  |         |         |         |         |         | 859.70   | 863.40  | 863.63  |
|  |         |         |         |         |         | 863.84   | 864.02  | 885.30  |
|  |         |         |         |         |         | 893.48   | 895.60  | 900.06  |
|  |         |         |         |         |         | 914.72   | 915.19  | 916.70  |
|  |         |         |         |         |         | 918.46   | 937.41  | 939.08  |
|  |         |         |         |         |         | 939.60   | 939.83  | 990.29  |
|  |         |         |         |         |         | 990.34   | 990.51  | 990.67  |
|  |         |         |         |         |         | 999.98   | 1000.41 | 1000.47 |
|  |         |         |         |         |         | 1000.89  | 1005.34 | 1006.84 |
|  |         |         |         |         |         | 1015.02  | 1018.10 | 1018.61 |
|  |         |         |         |         |         | 1018.86  | 1019.11 | 1021.18 |
|  |         |         |         |         |         | 1026.71  | 1035.79 | 1038.24 |
|  |         |         |         |         |         | 1044.17  | 1059.83 | 1063.17 |
|  |         |         |         |         |         | 1064.06  | 1072.66 | 1099.86 |
|  |         |         |         |         |         | 1100.67  | 1103.43 | 1104.19 |
|  |         |         |         |         |         | 1104.56  | 1105.12 | 1106.06 |
|  |         |         |         |         |         | 1112.07  | 1183.69 | 1183.79 |
|  |         |         |         |         |         | 1183.92  | 1184.09 | 1197.37 |
|  |         |         |         |         |         | 1205.87  | 1206.05 | 1206.13 |
|  |         |         |         |         |         | 1206.37  | 1233.61 | 1237.02 |
|  |         |         |         |         |         | 1262.56  | 1266.88 | 1271.44 |
|  |         |         |         |         |         | 1291.14  | 1305.15 | 1322.89 |
|  |         |         |         |         |         | 1323.55  | 1323.96 | 1328.30 |
|  |         |         |         |         |         | 1329.30  | 1331.94 | 1352.74 |
|  |         |         |         |         |         | 1358.41  | 1359.53 | 1359.64 |
|  |         |         |         |         |         | 1359.97  | 1363.82 | 1371.18 |
|  |         |         |         |         |         | 1372.96  | 1374.74 | 1395.95 |
|  |         |         |         |         |         | 1463.47  | 1466.11 | 1480.27 |
|  |         |         |         |         |         | 1481.46  | 1481.63 | 1481.66 |
|  |         |         |         |         |         | 1485.80  | 1496.42 | 1525.22 |
|  |         |         |         |         |         | 1530.21  | 1533.27 | 1536.15 |
|  |         |         |         |         |         | 1536.73  | 1539.14 | 1541.25 |
|  |         |         |         |         |         | 1550.50  | 1579.51 | 1579.89 |
|  |         |         |         |         |         | 1580.67  | 1600.83 | 1629.68 |
|  |         |         |         |         |         | 1630.33  | 1630.69 | 1631.02 |
|  |         |         |         |         |         | 1655.32  | 1656.17 | 1656.40 |
|  |         |         |         |         |         | 1657.09  | 2220.81 | 3164.55 |
|  |         |         |         |         |         | 3164.89  | 3164.92 | 3164.96 |
|  |         |         |         |         |         | 3175.51  | 3175.89 | 3175.92 |
|  |         |         |         |         |         | 3176.12  | 3188.44 | 3188.90 |
|  |         |         |         |         |         | 3188.98  | 3189.14 | 3198.92 |
|  |         |         |         |         |         | 3200.01  | 3201.01 | 3201.19 |
|  |         |         |         |         |         | 3204.55  | 3204.58 | 3206.37 |
|  |         |         |         |         |         | 3207.04  | 3251.58 | 3253.84 |
|  |         |         |         |         |         | 3256.62  | 3257.48 | 3271.30 |
|  |         |         |         |         |         | 3273.39  | 3276.52 | 3276.91 |

## Supporting Information Figure Captions

Figure S1. ORTEP diagram of asymmetric unit of  $[K(222)][Fe(TPP)(CN)]$  (100 K) displaying the atom labeling scheme. Thermal ellipsoids of all atoms are contoured at the 50% probability level. Hydrogen atoms have been omitted for clarity.

Figure S2. ORTEP diagram of the  $[Fe(TPP)(CN)]^-$  anion in  $[K(222)][Fe(TPP)(CN)]$  (100 K) displaying the atom labeling scheme. Thermal ellipsoids of all atoms are contoured at the 50% probability level. Hydrogen atoms have been omitted for clarity.

Figure S3. ORTEP diagram of asymmetric unit of  $[K(222)][Fe(TPP)(CN)]$  (296 K) displaying the atom labeling scheme. Thermal ellipsoids of all atoms are contoured at the 50% probability level. Hydrogen atoms have been omitted for clarity.

Figure S4. ORTEP diagram of the  $[Fe(TPP)(CN)]^-$  anion in  $[K(222)][Fe(TPP)(CN)]$  (296 K) displaying the atom labeling scheme. Thermal ellipsoids of all atoms are contoured at the 50% probability level. Hydrogen atoms have been omitted for clarity.

Figure S5. ORTEP diagram of asymmetric unit of  $[K(222)][Fe(TPP)(CN)]$  (325 K) displaying the atom labeling scheme. Thermal ellipsoids of all atoms are contoured at the 50% probability level. Hydrogen atoms have been omitted for clarity.

Figure S6. ORTEP diagram of the  $[Fe(TPP)(CN)]^-$  anion in  $[K(222)][Fe(TPP)(CN)]$  (325 K) displaying the atom labeling scheme. Thermal ellipsoids of all atoms are contoured at the 50% probability level. Hydrogen atoms have been omitted for clarity.

Figure S7. ORTEP diagram of asymmetric unit of  $[K(222)][Fe(TPP)(CN)]$  (400 K) displaying the atom labeling scheme. Thermal ellipsoids of all atoms are contoured at the 50% probability level. Hydrogen atoms have been omitted for clarity.

Figure S8. ORTEP diagram of the  $[Fe(TPP)(CN)]^-$  anion in  $[K(222)][Fe(TPP)(CN)]$  (400 K) displaying the atom labeling scheme. Thermal ellipsoids of all atoms are contoured at the 50% probability level. Hydrogen atoms have been omitted for clarity.

Figure S9. Formal diagram of the porphyrin cores of  $[K(222)][Fe(TPP)(CN)]$  structures at four different temperatures. Averaged values of the chemically unique bond distances (in Å) and angles (in degrees) are shown. The numbers in parentheses are the esd's calculated on the assumption that the averaged values were all drawn from the same population. The perpendicular displacements (in units of 0.01 Å) of the porphyrin core atoms from the 24-atom mean plane are also displayed. The positive values are towards the cyanide ligand positions.

Figure S10. Formal diagram of the porphyrin cores of  $[K(222)][Fe(TPP)(CN)]$  structures at four different temperatures. Averaged values of the chemically unique bond distances (in Å) and angles (in degrees) are shown. The numbers in parentheses are the esd's calculated on the assumption that the averaged values were all drawn from the same population. The perpendicular displacements (in units of 0.01 Å) of the porphyrin core atoms from the 4-atom mean plane are also displayed. The positive values are towards the cyanide ligand positions.

Figure S11. Selected Mössbauer spectra of  $[K(222)][Fe(TPP)(CN)]$  in 500mT field.

Figure S12. Temperature dependence of  $\chi_M T$  for  $[K(222)][Fe(TPP)(CN)]$  at two different magnetic field of 2000 and 20000 Gauss.

Figure S13.  $\chi_M T$  vs.  $T$  plot for  $[K(222)][Fe(TPP)(CN)]$  with temperature decreasing (400 → 2 K) and increasing (2 → 400 K) at magnetic field of 20000 Gauss.

Figure S14. Spin state energetics as a function of temperature, references to the LS state. This temperature dependence is explicitly due to the gas-phase entropy,  $S(\text{gas})$ . At no point does the IS state become thermodynamically favored over both the LS and HS states.

Figure S15. Multi-temperature (cooling from 296 to 105 K) measured IR spectra. Only  $C\equiv N$  stretches are showed for clarity.  $\nu_{C\equiv N}$  at 2070 and 2105  $\text{cm}^{-1}$  are correlated to LS and HS states respectively (  $\nu_{C\equiv N}$  at 2025 and 2040  $\text{cm}^{-1}$  are correlated to isotopic stretches of  $^{13}\text{C}\equiv ^{14}\text{N}$  and  $^{12}\text{C}\equiv ^{15}\text{N}$  ).

## Supporting Information Table Captions

Table S1. Complete Crystallographic Details for [K(222)][Fe(TPP)(CN)] at 100, 296, 325 and 400 K.

Table S2. Selected Structural Parameters for [K(222)][Fe(TPP)(CN)] at 100, 296, 325 and 400 K.

Table S3. Mössbauer Parameters of [K(222)][Fe(TPP)(CN)].

Table S4. Calculated and crystallographic structural parameters for the three spin-states.

Table S5. Optimized Cartesian coordinates for the low-, intermediate-, and high-spin structures.

Table S6. Unscaled frequencies for the optimized low-, intermediate-, and high-spin structures.